ORIGINAL PAPER

Thermal stress, cooling-rate and fictive temperature of silicate melts

Sharon L. Webb[1]

Abstract

The unknown cooling-rate history of natural silicate melts can be investigated using differential scanning heat capacity measurements together with the limiting fictive temperature analysis calculation. There are a range of processes occurring during cooling and re-heating of natural samples which influence the calculation of the limiting fictive temperature and, therefore, the calculated cooling-rate of the sample. These processes occur at the extremes of slow cooling and fast quenching. The annealing of a sample at a temperature below the glass transition temperature upon cooling results in the subsequent determination of cooling-rates which are up to orders of magnitude too low. In contrast, the internal stresses associated with the faster cooling of obsidian in air result in an added exothermic signal in the heat capacity trace which results in an over-estimation of cooling-rate. To calculate cooling-rate of glass using the fictive temperature method, it is necessary to create a calibration curve determined using known cooling- and heating-rates. The calculated unknown cooling-rate of the sample is affected by the magnitude of mismatch between the original cooling-rate and the laboratory heating-rate when using the matched cooling-/heating-rate method to derive a fictive temperature/cooling-rate calibration curve. Cooling-rates slower than the laboratory heating-rate will be overestimated, while cooling-rates faster than the laboratory heating-rate are under-estimated. Each of these sources of error in the calculation of cooling-rate of glass materials—annealing, stress release and matched cooling/heating-rate calibration—can affect the calculated cooling-rate by factor of 10 or more.

Keywords Fictive temperature · Annealing · Thermal stress · Cooling-rate · Calorimetry

Introduction

The cooling-rate history of silicate melts can be investigated using differential scanning heat capacity measurements together with the fictive temperature analysis method of Tool (1946), Narayanaswamy (1971) and Moynihan et al. (1976). Studies of the limiting fictive temperature and the cooling-rate of synthetic and natural glasses using this method are increasingly found in the literature (e.g. Moynihan et al. 1976; De Bolt et al. 1976; Wilding et al. 1995; Webb 2008; Potuzak et al. 2008; Guo et al. 2011 and more recently Helo et al. 2013; Hui et al. 2018). Synthetic silicate melts have been used in a number of studies to illustrate the robustness of this method of limiting fictive temperature determination

✉ Sharon L. Webb
  swebb@gwdg.de

1   Mineralogy Department, Georg-August University, Goettingen, Germany

using the "equal area" method described by Moynihan et al. (1976). Cooling- and heating-rates of 80–2 K min^{-1} have been used (e.g. Moynihan et al. 1976; Yue et al. 2002). These heating-rates are a function of the intrinsic properties of the calorimeter furnace and the size of the sample.

There are a number of studies which address the calculation of the limiting fictive temperature of micrometre sized hyper-quenched glasses. In all cases, there is a problem in calculating the heat capacity of the glass due to the large exothermic enthalpy release at temperatures hundreds of degrees below the glass transition peak in the calorimetry data. The method of Yue et al. (2002) overcomes the difficulty in determining the heat capacity of the glass upon the first heating by taking the data from the second heating together with T_g calculated from the intercept of the slopes of straight lines fitted to the glassy heat capacity and the rising peak of the second heating run.

Guo et al. (2011) addressed the same problem using the fictive temperature T_{f2} determined by the equal area technique on matched cooling- and heating-rate data, instead of T_g, to define the temperature limit of the integral needed

to determine the limiting fictive temperature T_{f1} from the heat capacity measured in the first heating run of hyper-quenched glass.

These studies are interested in the thermodynamics of determining the limiting fictive temperature of the starting material to study changes in physical properties with fictive temperature. The fictive temperature can, however, be used to determine the rate at which the sample was cooled through the glass transition. This cooling-rate information is needed to address the position of an obsidian in a lava flow or magma chamber; the effects of re-charging hot magma in a magma chamber (e.g. Ginibre et al. 2002); the annealing of obsidians during ascent (e.g. Rust et al. 2004); and to address the production methods of historical glasses from archaeological settings. This leads to the need to perform heat capacity measurements at heating-rates similar to those used by Moynihan and his research colleagues 2–80 K min^{-1} as these rates cover most the expected range of cooling-rates for centimetre to metre sized glasses in both geological and anthropological settings—except for the cases of very slow cooling and annealing in magma chambers and conduits (Rust et al. 2004) and very fast cooling (hyper-quenching) of thin glass flakes from pillow lavas underwater (Potuzak et al. 2008).

Here, we investigate three different features of the experimental technique in which the unknown cooling-rate history of silicate melts can be investigated using differential scanning heat capacity measurements together with the fictive temperature analysis method of Tool (1946), Narayanaswamy (1971) and Moynihan et al. (1976).

1. In their development of the equations to describe limiting fictive temperature (T_f), Moynihan et al. (1974) discussed the need to have matched cooling- and heating-rate data in order that a plot of $-\log_{10}$ |cooling-rate| against $1/T_f$ would have the same slope as a plot of $\log_{10}$ viscosity against $1/T$ (T is temperature in K). This was based on the assumption that the relaxation rate of the melt structure was a function of the viscosity of the melt. The relationship between the lifetime of Si–O bonds, viscosity and structural relaxation has now been established over 8 orders of magnitude from 10^{-6} to 10^2 s (e.g. Dingwell and Webb 1990; Webb, 1992; Farnan and Stebbins 1994) with Yue et al. (2004) confirming this relationship for quench-rate and viscosity. Subsequent discussions of the use of the fictive temperature analysis has led to the need to differentiate between the fictive temperature $T_f(T)$ which is temperature dependent, equal to the ambient temperature and is the temperature at which the melt structure is in thermal equilibrium, and the limiting fictive temperature T_f' which is that frozen in upon cooling and is independent of temperature and

is the temperature (upon cooling) at which the melt structure ceased to be in thermal equilibrium. The limiting fictive temperature is independent of the subsequent heating-rate, however, if the equal area method of Tool-Narayanaswamy-Moynihan is used with unmatched cooling- and subsequent heating-rates, an incorrect or false fictive temperature will be calculated.

Here, we investigate the effect of breaking away from the Moynihan et al. (1976) method of determining the limiting fictive temperature in which matching cooling- and subsequent heating-rates are used. A constant heating-rate is used for a series of different cooling-rates to produce a "false limiting fictive temperature" which is given here the symbol F_f', calculated using the equal area method. A plot of $-\log_{10}$ |cooling-rate| against inverse false limiting fictive temperature has a different slope to that plotted against the inverse of the limiting fictive temperature.

This approach is especially important when one wants to determine the unknown cooling-rate of a glass but does not want to discuss either the glass structure or the fictive temperature—as defined by Narayanaswamy (1971) and Moynihan et al. (1974). As the cooling-rate of the glass is unknown, it is not possible to determine the real limiting fictive temperature using a heating-rate that is the same as the cooling-rate of the sample. The importance of this difference in heating- and cooling-rate is investigated here using scanning heat capacity measurements.

2. In practice, in such calorimetry studies of quenched natural or synthetic glasses, it is observed that the unrelaxed heat capacity curve obtained in the first heating cycle is relatively noisy and results in unrelaxed, glass heat capacity values slightly less than those of the subsequent heating measurements. In many cases, there appears to be a large exothermic reaction at ∼ 400 C (Note: the majority of published heat capacity traces for glasses show endothermic reactions as positive). This exothermic signal is only observed in the first heating of the sample to temperature above the glass transition. Here, we investigate the heat capacity for a range of silicate melts, and discuss reasons for the difference between the first heat capacity determination of a melt sample cooled in air by taking the crucible out of the furnace and the subsequent controlled cooling.

3. In the course of investigating the different heating and cooling effects on the limiting fictive temperature determined from the equal area method of analysing the heat capacity curve, we also investigated the effect of annealing on the calculated limiting fictive temperate.

Previous studies have discussed the physical meaning of the fictive temperature and that it is the temperature at which

the melt structure was in equilibrium with temperature as the melt cooled; and that this is related to the structural relaxation time which in turn controls the viscosity of the melt (e.g. Narayanaswamy 1971; Moynihan et al. 1976). Here, we will knowingly step away from the strict meaning of fictive temperature and use the false fictive temperature to obtain productive information about the unknown cooling-rate of silicate melts. The method of Yue et al. (2002) and later Guo et al. (2011) allows the determination of the limiting fictive temperature of a glass despite the unmatched cooling- and heating-rates experienced by the glass; but does not tell us the cooling-rate experienced by the glass.

Experiments

Melt synthesis

A series of melts were synthesized from powdered oxides and carbonates. The powders were dried at 150 C for 24 h and the MgO powder was fired at 1000 °C to remove the CO_2 and H_2O, before being weighed in to the $Pt_{90}Rh_{10}$ crucible used to de-carbonate at 1000 °C overnight. The melts were synthesized at 1600 °C. The samples were melted, crushed and re-melted twice to produce a bubble-free glass of homogeneous composition. The melts were quenched to a glass by immersing the crucible in water until the glass was ~ 100 °C.

Six glasses were synthesised. The samples consisted of 3 peralkaline glasses: a standard container glass and a window glass composition and a glass with the NIQ composition of Whittington et al. (2000) together with 3 metaluminous glasses: two Fe-free haplo-analogs of the foiditic magmas from the Colli Albani Volcanic District; H. Rosse-Pozzolane

Rossi (Freda et al. 2011), and H. Nere-Pozzolane Nere (Campagnola et al. 2016) and a basalt (Webb et al. 2014). The composition of the glasses was determined by electron microprobe and the analyses are given in Table 1. The polymerisation of the melts is calculated in terms of NBO/T (Mysen 1987) and peraluminosity—the γ-term (Zimova and Webb 2006) as shown in Table 1; where

$$\gamma = \frac{Na_2O + K_2O + CaO + MgO + FeO}{Na_2O + K_2O + CaO + MgO + FeO + Fe_2O_3 + Al_2O_3}$$

(1)

for melt composition in mole fraction.

Calorimetry

The heat capacity of the glasses and melts was determined by differential scanning calorimetry methods using a Netzsch® DSC 404C. Heating- and cooling-rates in the range 35–2 K min⁻¹ are used. The glass samples are cylinders, 6 mm in diameter and 1.6 mm thick with polished parallel ends. The calorimeter is calibrated using a single crystal of sapphire. The heat capacity of sapphire is taken from Robie et al. (1978). The heat capacity of the glass samples is measured against the second empty crucible. The furnace is flushed with argon gas. An endothermic signal is seen upon heating through the glass transition as the melt structure relaxes into thermodynamic equilibrium.

Fictive temperature

As shown by Moynihan et al. (1974),…" *the dependence of the glass transition temperature T_g on heating or cooling-rate |q| is given to a high degree of approximation by*

Table 1 Chemical compositions of the investigated melts determined by electron microprobe analysis (JEOL JXA 8900 RL) with 15 kV acceleration voltage, 15 nA current and 25 μm beam diameter

Mol%	Container glass	NIQ	H. Rosse	H. Nere	Window glass	Basalt
SiO_2	73.97	42.81	51.26	60.04	68.79	54.79
Al_2O_3	1.42	5.92	13.26	14.94	0.78	9.77
TiO_2	0.01	2.2	0.85	0.58	0.01	1.10
Na_2O	13.72	7.43	3.44	2.86	12.77	2.75
K_2O	0.01	0.64	6.69	6.92	0.01	0.21
CaO	10.83	27.65	13.29	6.91	7.91	12.46
MgO	0.02	13.33	11.29	7.75	9.73	13.81
FeO						1.10
Fe_2O_3						3.82
Γ	0.95	0.89	0.72	0.62	0.98	0.69
NBO/T	0.60	1.52	0.55	0.21	0.84	0.40

Listed data are the average of 10 single measurements. The basalt composition is taken from Webb et al. (2014) as it is from the same glass batch

γ = (Na_2O + K_2O + CaO + MgO + FeO)/(Na_2O + K_2O + CaO + MgO + FeO + Fe_2O_3 + Al_2O_3)

NBO/T = (2 O – 4 T)/T

$$\frac{d \ln |q|}{d(1/T_g)} = -\Delta h * /R, \tag{2}$$

where $\Delta h*$ is the activation enthalpy for the relaxation times controlling the structural enthalpy or volume relaxation. The conditions necessary for the validity of these relations are that the structural relaxation be describable by a temperature-independent distribution of relaxation times and that the glass be cooled from a starting temperature well above the transition region and subsequently reheated at the same rate starting from a temperature well below the transition region.......$\Delta h*$ is found to be equal within experimental error to the activation enthalpy for the shear viscosity". The glass transition temperature, T_g, in this equation is defined as some characteristic temperature on the heat capacity curve. Narayanaswamy (1988) showed this equation to be exact, and not just a "good approximation".

With increasing development of the equations describing structural relaxation, the term T_g was replaced by limiting fictive temperature T_f', (Narayanaswamy 1971) with the definition of T_f being the temperature at which the glass structure would be in thermodynamic equilibrium and limiting fictive temperature being that frozen in upon cooling (the temperature at which the melt structure was in thermal equilibrium). Narayanaswamy (1971) and Moynihan et al. (1976) expanded the use of Eq. 2 based upon the relationship between the temperature-dependent heat capacity and the temperature-dependent fictive temperature:

$$\frac{dT_f}{dT}\bigg|_T = \frac{\left[C_p(T) - C_{pg}(T)\right]\big|_T}{\left[C_{pe}(T) - C_{pg}(T)\right]\big|_{T_f}} \tag{3}$$

$$\Rightarrow \int_{T'}^{T*} \left[C_p(T) - C_{pg}(T)\right] dT = \int_{T_f'}^{T*} \left[C_{pe}(T) - C_{pg}(T)\right] dT_f \tag{4}$$

(DeBolt et al. 1976) for T_f—fictive temperature, T temperature in K, C_p—heat capacity as a function of temperature, C_{pg}—unrelaxed (glassy) heat capacity as a function of temperature, C_{pe}—relaxed heat capacity as a function of temperature; with T_f'—limiting fictive temperature, and $T*$—a temperature above the glass transition region at which the heat capacity is equal to the equilibrium heat capacity, T'—a temperature below the glass transition region at which the heat capacity is that of the unrelaxed glass. Equation 4 is shown graphically in Fig. 1. The unrelaxed glass heat capacity is extrapolated by ~ 150 C to higher temperature using the Maier-Kelley equation (Maier and Kelley 1932):

$$C_{pg}(T) = a + bT + cT^{-2} \tag{5}$$

for T in K.

Results and discussion

The limiting fictive temperature of the container glass and also the NIQ glass has been determined for matched cooling- and heating-rates of 2, 5, 10, 15, 20, 25, 30 and 35 K min^{-1}; and the false fictive temperature has been determined for a heating-rate of 20 K min^{-1} with unmatched cooling-rates. The heat capacity curves for the container glass are shown in Fig. 2

Figure 2 illustrates the heat capacity data for the container glass for both matched and unmatched (moved 200 C to the right in this diagram) cooling- and heating-rates, together
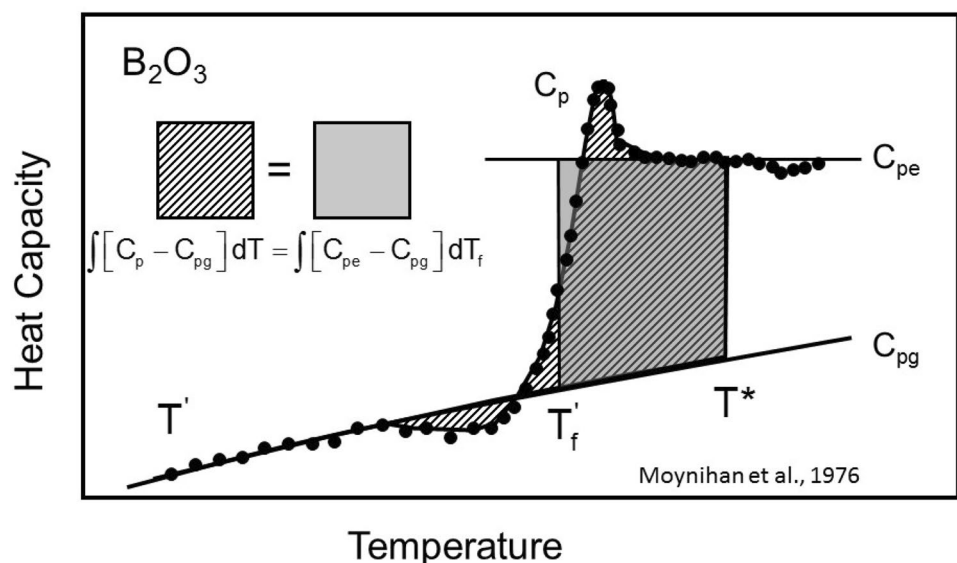
Fig. 1 Graphical representation of Eq. 3, as found in Moynihan et al. 1976, showing the two integrals which need to equal to each other to determine the limiting fictive temperature T_f'. The choice of $T*$ and T' depends upon the cooling history of the sample; for rapidly quenched samples, T' is much lower than the temperature of the peak in the heat capacity data to allow for the $C_p(T)$ curve below the C_{pg} curve. This results in $T*$ being much larger than the temperature of the peak in the C_p curve to counterbalance the large negative part of the integral

Fig. 2 Heat capacity data for container glass with matched and unmatched cooling- and heating-rates, together with curves for melts which had been cooled and heated at 20 K min^{-1} but annealed upon cooling from above the glass transition temperature at 490 C, 475 C and 380 C for 6 h. The unmatched rate data have been shifted along the X-axis to the right by 200 C; and the data for the annealed samples have been shifted to the left by 200 C. The cooling-rates are indicated; as are the annealing temperatures
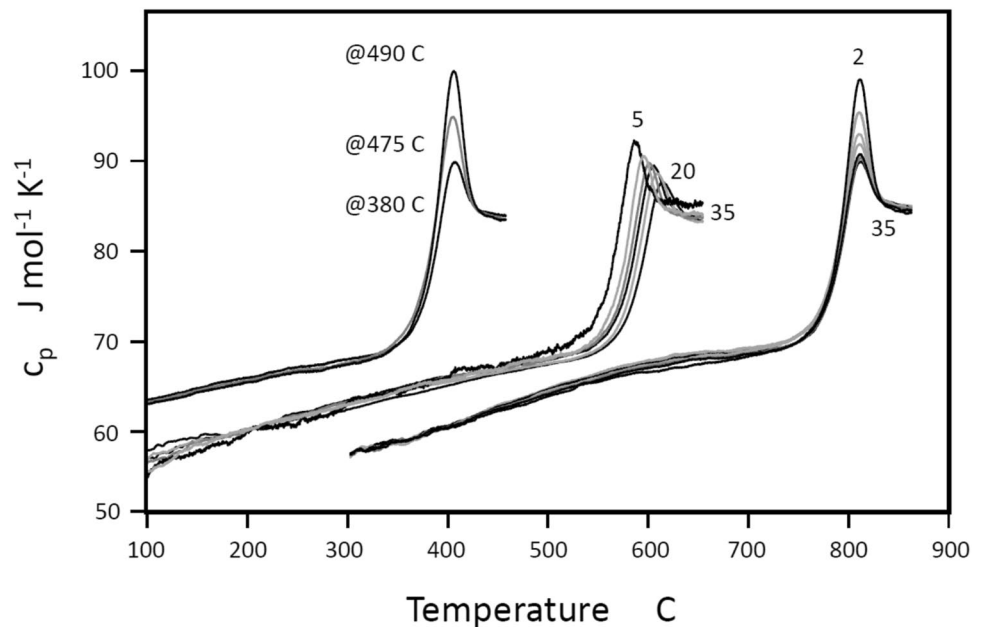
with data for annealed glasses (moved 200 C to the left in this diagram). As expected, the endothermic glass transition peak becomes smaller and moves to higher temperature with faster matched cooling- and heating-rates. In comparison, the unmatched cooling-rate data obtained for a heating-rate of 20 K min^{-1} show a peak whose position remains independent of temperature (over the range of cooling-rates) but decreases with increasing cooling-rate. In a third series of experiments, the heat capacity curve was also determined at 20 K min^{-1} heating-rate for a piece of container glass which had been cooled from above the glass transition with 20 K min^{-1} and then annealed at 490 C for 6 h before being cooled to room temperature. The same piece of glass was cooled from above the glass transition and annealed at 475 C for 6 h; in a third run, the glass was held at 380 C for 6 h after being cooled at 20 K min^{-1} from above the glass transition temperature. The height of the glass transition peak is greater for the annealed samples than for the glass which was heated to above the glass transition and simply cooled at 20 K min^{-1}.

The limiting fictive temperature T'_f and the false limiting fictive temperature F'_f for the matched and unmatched cooling- and heating-rate conditions, respectively, were determined for the container glass and the NIQ glass using Eq. 4, and are given in Table 2 and shown in Fig. 3. The limiting fictive temperatures determined from the unmatched heat capacity data using the unified method of Guo are also given in Table 2.

A plot of $-\log$ |cooling-rate| against inverse temperature shows two different straight lines (Arrhenian fits) for the matched and unmatched cooling–heating-rate measurements. This illustrates the need to determine unknown cooling-rates with the unmatched calibration method. An alternative method would be to use the Guo et al. (2011) analysis method to determine the limiting fictive temperature of the unknown sample independent of heating-rate; and then to create a calibration curve using the same technique or the equal area/equal cooling- and heating-rate method of Moynihan to determine the unknown cooling-rate of the sample.

As illustrated in Fig. 3, there is easily a factor of 2 difference in the cooling-rate calculated from the fictive temperature, depending upon which calibration curve is used; with unmatched cooling-rates slower than the 20 K min^{-1} heating-rate used here being overestimated and cooling-rates faster than 20 K min^{-1} being underestimated by up to a factor of 2 over the present 2–35 K min^{-1} cooling-rate range. Extrapolation of the straight-line calibration will increase the over- and under-estimation of the cooling-rate when using the matched cooling-/heating-rate calibration curve.
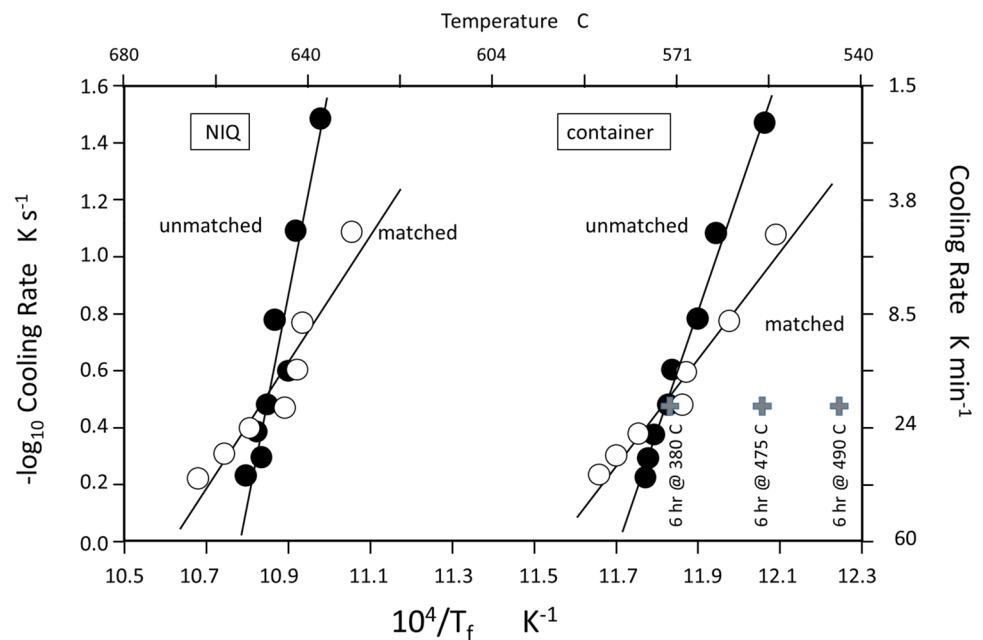
Annealing

The limiting fictive temperature has also been calculated for the container glass that had been annealed upon cooling. This measurement was performed on a piece of glass that had been heated to above the glass transition temperature and then cooled at 20 K min^{-1}, held at a fixed temperature for 6 h and then cooled to room temperature with 20 K min^{-1}. As seen in Fig. 3, the cooling-rate of annealed sample is underestimated (cooling-rates slower than 20 K min^{-1} are calculated). The annealed samples can be easily identified from their heat capacity data as the glass transition peak is higher than that obtained when the sample was cooled and heated

Table 2 Limiting fictive temperature T'_f and false limiting fictive temperature F'_f for container glass and NIQ glass

Cooling-rate	Container glass			NIQ		
	Matched heating rate	20 K min⁻¹ heating rate	Unified approach	Matched heating rate	20 K min⁻¹ heating rate	Unified approach
K min⁻¹	T'_f (C)	F'_f(C)		T'_f (C)	F'_f(C)	
2	–	555.75	544.7	–	638.25	623.6
5	553.50	564.25	557.6	631.25	643.25	635.9
10	561.75	567.00	564.5	642.00	648.00	643.7
15	569.00	571.25	570.9	642.50	644.50	643.7
20	570.25	572.25	571.3	645.25	648.25	–
25	577.50	575.25	576.6	651.50	651.00	653.6
30	582.00	575.75	580.0	657.75	649.75	653.4
35	584.50	576.75	582.4	663.50	652.75	657.9
Annealed 6 h	A'_f					
490 C	543.5		568.2			
475 C	555.5		573.3			
380 C	570.5					

The calculated limiting fictive temperature of the annealed glass (A'_f) are also given. The limiting fictive temperature was also determined from the unmatched cooling-/heating-rate data using the unified approach of Gou et al. (2011). The calculated error in temperature is ± 2 K

Fig. 3 $-\log$ |cooling-rate| as a function of inverse calculated limiting fictive temperature for matched cooling- and heating-rates (hollow symbols) and unmatched cooling- and heating-rates (black symbols) for NIQ melt and container glass melt. The plus signs are for melt cooled at 20 K min⁻¹ from above the glass transition temperature and then held at 380 C, 475 C and 490 C for 6 h before being cooled to room temperature at 20 K min⁻¹. Straight lines have been fit to the data

without annealing at a rate of 20 K min⁻¹ (see Fig. 2). The limiting fictive temperature calculated for the sample which had been annealed at 380 C is the same as that of a sample cooled from above the glass transition at 20 K min⁻¹. This indicates that the annealing temperature was too low to allow for structural relaxation to occur over the 6 h of the anneal. The correct limiting fictive temperature of the annealed sample could be calculated using the two-measurement unified approach of Guo et al. (2011). The comparison of the false

fictive temperature and the corrected value obtained using this technique would immediately show that the glass had been annealed for some time at an unknown temperature.

Thermal stress

All methods of determining the real or false fictive temperature rely on extrapolating the glass heat capacity to temperatures above the glass transition. Figure 4 shows the
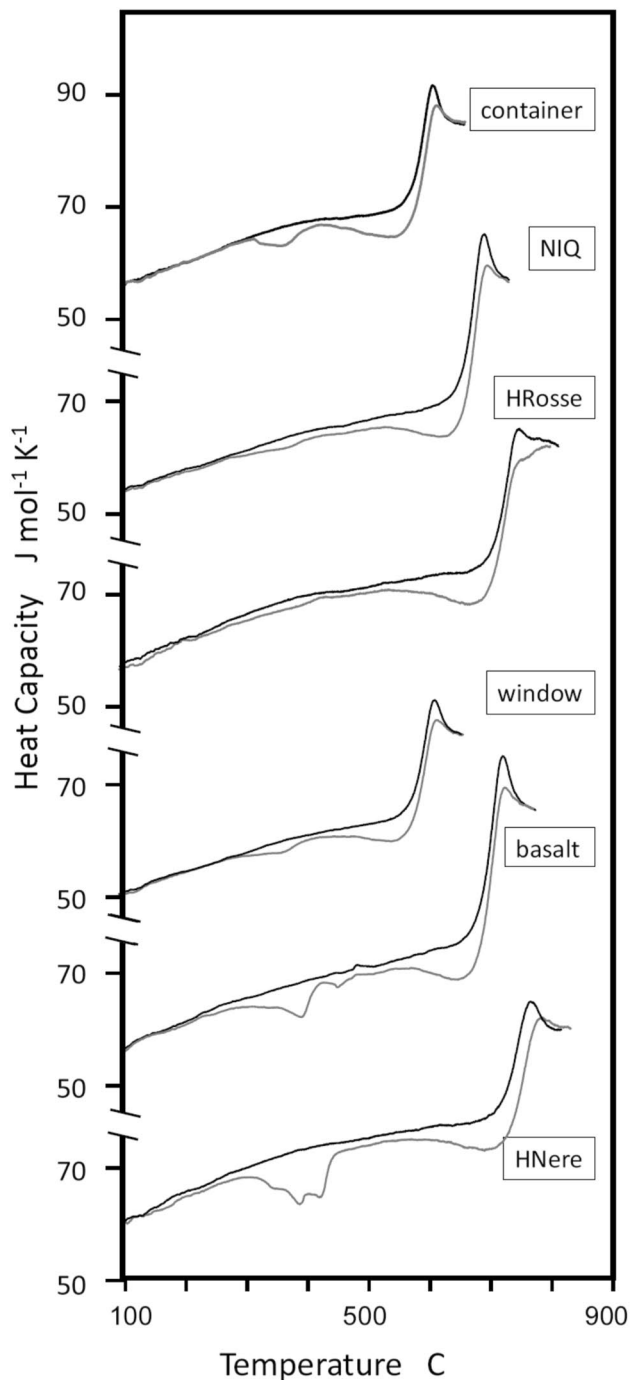
Fig. 4 The heat capacity calculated from first (unknown cooling-rate and 20 K min^{-1} heating-rate) and second (20 K min^{-1} cooling- and heating-rate) heating curves for each of the glasses studied

heat capacity determined in the first and second heating runs for all six glasses. Four of the six glasses investigated here show an exothermic signal in the heat capacity measurement. This signal is restricted to the temperature range 300–450 C. This exothermic signal is only seen in the first heating of the glass. All of the glass samples (except for the black basalt glass) show optical birefringence before the first heating cycle but not afterwards. These heat capacity traces are similar to those of Johari (2014) in which the low temperature exotherm due to stress release and the high temperature exotherm due to structural relaxation are discussed. These three observations would imply that the exothermic signal in the present glasses is due to the release of energy as the stress which was frozen in to the glass structure upon cooling through the glass transition is released.

The birefringence observed in silicate glasses which have stress induced structural anisotropy has been discussed in the literature (e.g. Murach et al. 1997; Hausmann et al. 2020). The samples in these studies were in general, glass fibres forced through nozzles and deformed as they cooled though the glass transition. Johari (2014) pointed out that these thermal stresses decrease (relax) at a faster rate (lower temperatures) than the glass structure relaxes to the equilibrium state (the glass transition). Thus, it would appear that the present samples were exposed to high differential stress as they cooled through the glass transition. This mechanical stress produced an anisotropic structure frozen in to the glass. This anisotropy is seen as birefringence. These melts were cooled by taking the crucible out of the furnace and setting it on an alumina plate to cool to room temperature.

It is assumed that these thermal stresses occur in the present melts due to the surface of the melt in the crucible cooling quickly and producing a fixed volume of melt, with the interior cooling more slowly inside this fixed volume. As the now cold interior has a smaller volume than the originally hot interior, but is fixed inside the original shell, we have a glass shell in compression and an interior in tension.

This exothermic stress release signal should not be included in the calculation of limiting fictive temperature using Eq. 4. The exotherm seen at temperatures above 500 C is a function of the cooling-rate and heating-rate of the sample. The exotherm occurring at temperatures below 500 C is assumed to be due to the release of stress which was built into the sample as it cooled.

In the case of the container glass, fitting the Meier–Kelley equation to the original data set, but not including the first low-temperature exotherm, gives a false limiting fictive temperature of 601 C. Taking the unmatched calibration curve for cooling-rate of this melt, this F'_f gives a cooling-rate of 10^3 K min^{-1}. If the glassy heat capacity curve from the second measurement is used for fitting the Meier–Kelley equation, the false limiting fictive temperature calculated from the original container glass heat capacity is 626 C and the cooling-rate is $10^{4.3}$ K min^{-1} (20,000 K min^{-1}). If the data from the second glass heat capacity curve is used for the Meier–Kelley fit, and both exotherms are included in the calculation, a false limiting fictive temperature of 637 C is calculated; giving a cooling-rate $10^{4.8}$ K min^{-1} (63,000 K min^{-1}). This would suggest that the choice of

Meier–Kelley fit for stressed glasses can result in a factor of ~20 overestimate in in the cooling-rate due to the exothermic effect of stress release in the first heating segment; with the inclusion of the low-temperature exotherm resulting in an overestimation of the cooling-rate by a factor of ~3. Thus, the effect of the low-temperature stress release as well as the continual stress release occurring in the first heating of the sample can result in the calculation of cooling-rates that are a factor of ~100 too fast. It is expected that this overestimation would increase for faster cooling conditions in which more thermal stress is built in to the sample. However, Guo et al. (2011) suggest that the excess energy stored in the glass due to thermal stresses is significantly smaller than the hyper-quenching excess energy and would thus influence the fictive temperature determined by the area matching method only to a limited extent.

Hyper-quench

There are also studies of the cooling-rate of glass insulation wool (e.g. Yue et al. 2002; Ya et al. 2008) and hyper-quenched obsidian flakes (Potuzak et al. 2008). Figure 5 illustrates the series of heating experiments for a piece of glass wool. Before being placed in the calorimeter, the wool sample was cleaned in methanol in an ultrasonic bath for 80 min and dried by heating to 40 C. Each heating- and subsequent cooling-rate was 20 K min^{-1}. In this study, the glass wool was heated to 660 C at 20 K min^{-1}, held there for 1 min and then cooled at 20 K min^{-1}. It is clear that the melt structure did not fully relax during the first—or the second heating excursion. The fourth and fifth heating run produced

the same heat capacity curve and, therefore, it is assumed that the melt relaxed to its thermal equilibrium structure during the third heating across the glass transition temperature. The data of Yue et al. (2002) and Helo et al. (2013) show the glass wool to have relaxed after the first heating run.

The first run shows the hyper quench-rate of the rock-wool, with the heat capacity peak being difficult to identify. The identification is made easier by comparison with subsequent heating. All five heating runs were done on the same sample which was left in the calorimeter between runs. The first heating illustrates an exothermal signal at ~200 C and then a much larger exothermal signal at ~400 C. The glass transition peak is seen to occur at ~580 C. The second and third runs show that the fictive temperature (structure) of the glass has not re-equilibrated. Thus despite being above the glass transition temperature, the sample requires more time to achieve structural equilibrium with temperature (e.g. Richet 2002). The fourth and fifth runs produce identical heat capacity curve, indicating the glass structure has equilibrated to that at 660 C.

Conclusion

To determine the unknown cooling-rate of synthetic and natural glass, it is suggested that a false limiting fictive temperature approach should be employed, as the cooling-rate is unknown and the sample cannot be heated at a matched rate. In the present range of cooling-rates, a factor of 5 in the overestimation and under-estimation of cooling-rates which were slower and faster, respectively, than the 20 K min^{-1}

Fig. 5 The heat capacity of rock-wool fibre determined in 5 sequential heating runs of 20 K min^{-1}. The first cooling-rate is unknown, all subsequent cooling-rates are 20 K min^{-1}
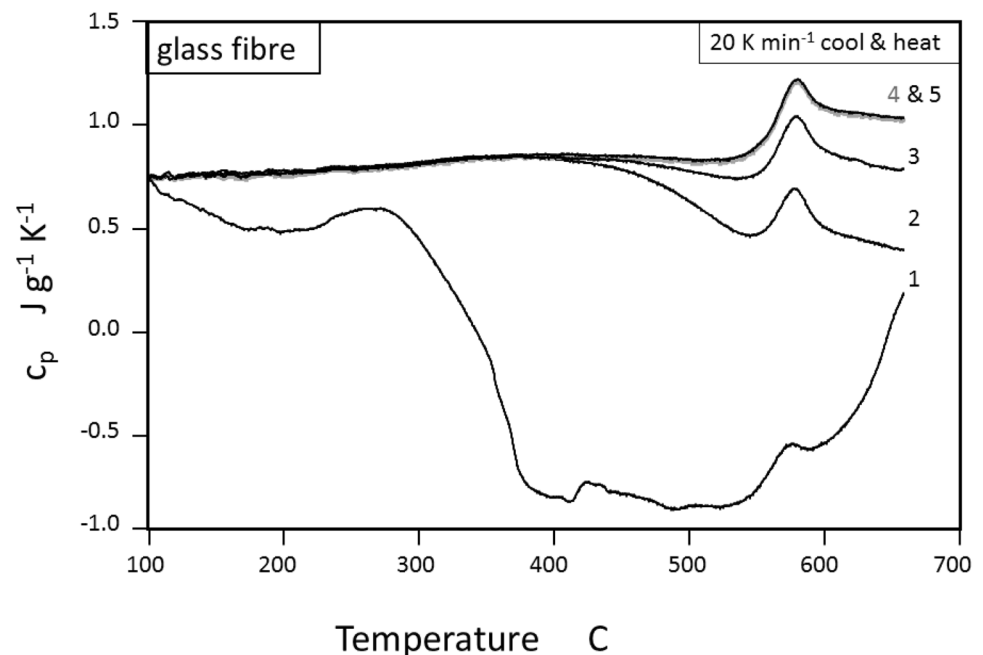
heating-rate is apparent. The effect of stress release on the heat capacity curve can result in an overestimation of the cooling-rate of the sample by up to orders of magnitude.

Declarations

Conflict of interest Not applicable.

Code availability Not applicable.

References

Bottinga Y, Sipp A, Richet P (2001) Time-dependent isothermal variations of silicate melt viscosity after sudden temperature or stress changes. J Non Cryst Sol 290:129–144

Campagnola S, Vona A, Giordano G (2016) Crystallization kinetics and rheology of leucite-bearing tephriphonolite magmas from the Colli Albani volcano (Italy). Chem Geol 424:12–29

DeBolt MA, Easteal AJ, Macedo PB, Moynihan CT (1976) Analysis of structural relaxation in glass using rate heating data. J Am Ceram Soc 59:16–21

Dingwell DB, Webb SL (1990) Relaxation in silicate melts. Europ J Mineral 2:427–449

Farnan I, Stebbins JF (1994) The nature of the glass transition in a silica-rich oxide melt. Science 265:1206–1209

Freda C, Gaeta M, Giaccio B, Marra F, Palladino DM, Scarlat P, Sottili G (2011) CO_2-driven large mafic explosive eruptions: the Pozzolane Rosse case study from the Colli Albani Volcanic District (Italy). Bull Volcanol 73:241–256

Ginibre C, Wörner G, Kronz A (2002) Minor- and trace-element zoning in plagioclase: implications for magma chamber processes at Parinacota volcano, northern Chile. Contrib Mineral Petrol 143:300–315

Guo X, Potuzak M, Mauro JC, Allan DC, Kiczenski TJ, Yue Z (2011) Unified approach for determining the enthalpic fictive temperature of glasses with arbitrary thermal history. J Non-Cryst Solid 357:3230–3236

Hausmann BD, Miller PA, Aaldenberg EM, Blanchet TA, Tomozawa M (2020) Modeling birefringence in SiO_2 glass fiber using surface stress relaxation. J Am Ceram Soc 103:1666–1676

Helo C, Clague DA, Dingwell DB, Stix J (2013) High and highly variable cooling-rates during pyroclastic eruptions on Axial Seamount, Juan de Fuca Ridge. J Volc Geotherm Res 253:54–64

Hui H, Hess KU, Zhang Y, Nichols ARL, Peslier AH, Lange RA, Dingwell DB, Neaf CR (2018) cooling-rates of lunar orange glass beads. Earth Planet Sci Lett 503:88–94

Johari GP (2014) Calorimetric features of release of plastic deformation induced internal stresses, and approach to equilibrium state on annealing of crystals and glasses. Thermochim Acta 58:14–25

Maier CG, Kelley KK (1932) An equation for the representation of high-temperature heat content data. J Am Chem Soc 54:3243–3246

Moynihan CT, Easteal AJ, Wilder J (1974) Dependence of the glass gransition gemperature on heating and cooling-rate. J Phys Chem 78:2673–2677

Moynihan CT, Easteal AJ, DeBolt MA, Tucker J (1976) Dependence of fictive temperature of glass on cooling-rate. J Am Ceram Soc 59:12–16

Murach J, Brückner R (1997) Preparation and structure-sensitive investigations on silica glass fibers. J Non Cryst Sol 211:250–261

Mysen BO (1987) Magmatic silicate melts: relationships between bulk composition, structure and properties. In: BO Mysen (editor) Magmatic processes: physicochemical principles. Special Publication No. 1, The Geochemical Society

Narayanaswamy OS (1971) Model of structural relaxation in glass. J Am Ceram Soc 54:491–498

Narayanaswamy OS (1988) Thermorheological simplicity in the glass transition. J Am Ceram Soc 71:900–904

Potuzak M, Nichols ARL, Dingwell DB (2008) Hyperquenched volcanic glass from Loihi Seamount Hawaii. Earth Planet Sci Lett 270:54–62

Richet P (2002) Enthalpy, volume and structural relaxation in glass-forming silicate melts. J Therm Anal Calorimetry 69:739–750

Robie RA, Hemingway BS, Fisher JR (1978) Thermodynamic properties of minerals and related substances at 298.15 K and 1 Bar (105 Pascals) pressure and at higher temperatures. US Geological Survey Bulletin, Washington

Rust AC, Cashman KV, Wallace PJ (2004) Magma degassing buffered by vapor flow through brecciated conduit margins. Geology 32:349–352

Tool AQ (1946) Relation between inelastic deformability and thermal expansion of glass in Its annealing range. J Am Ceram Soc 29:240–253

Webb SL (1992) Shear, volume, enthalpy and structural relaxation in silicate melts. Chem Geol 96:449–457

Webb SL (2008) Configurational heat capacity of Na_2O-CaO-Al_2O_3-SiO_2 melts. Chem Geol 256:92–101

Webb SL, Bramley J, Murton A, Wheeler J (2014) Rheology and the Fe^{3+}–chlorine reaction in basaltic melts. Chem Geol 366:24–33

Whittington A, Richet P, Holtz F (2000) Water and the viscosity of depolymerized aluminosilicate melts. Geochim Cosmochim Acta 64:3725–3736

Wilding MC, Webb SL, Dingwell DB (1995) Evaluation of a relaxation geospeedometer for volcanic glasses. Chem Geol 125:151–160

Ya M, Deubener J, Yue Y (2008) Enthalpy and anisotropy relaxation of glass fibers. J Am Ceram Soc 91:745–751

Yue Y, von der Ohe R (2004) Jensen SL (2004) Fictive temperature, cooling-rate, and viscosity of glasses. J Chem Phys 120:8053–8059

Yue YZ, JdeC C, Jensen SL (2002) Determination of the fictive temperature for a hyperquenched glass. Chem Phys Lett 357:20–24

Zimova M, Webb SL (2006) The effect of chlorine on the viscosity of Na_2O-Fe_2O_3-Al_2O_3-SiO_2 melts. Am Mineral 91:344–352